

## Weak Alignment of Paramagnetic Proteins Warrants Correction for Residual CSA Effects in Measurements of Pseudocontact Shifts

Michael John,<sup>†</sup> Ah Young Park,<sup>†</sup> Guido Pintacuda,<sup>‡</sup> Nicholas E. Dixon,<sup>†</sup> and Gottfried Otting<sup>\*,†</sup>

Research School of Chemistry, Australian National University, Canberra, ACT 0200, Australia, and Laboratoire de Chimie, Ecole Normale Supérieure de Lyon, 46 Allée d'Italie, 69364 Lyon, France

Received September 23, 2005; E-mail: gottfried.otting@anu.edu.au

Paramagnetic metal ions with an anisotropic magnetic susceptibility  $\chi$  induce pseudocontact shifts (PCS) that can significantly change the chemical shifts of nuclear spins up to 40 Å from the metal ion.<sup>1</sup> PCSs represent a rich source of information for 3D structure determinations<sup>2</sup> and resonance assignments<sup>3</sup> of metalloproteins as they report on the location of the nuclear spin with respect to the  $\chi$  tensor:

$$\Delta\delta^{\text{PCS}} = \frac{1}{4\pi r^3} \sum_i \cos^2 \theta_i \Delta\chi_{ii} \quad (1)$$

where  $r$  is the metal–nuclear distance, and  $\cos \theta_i$  ( $i = x, y, z$ ) values are the three direction cosines of the metal–nuclear vector with respect to the Cartesian principal axes of the traceless part  $\Delta\chi$  of  $\chi$  with the components  $\Delta\chi_{ii}$ .

Recently, PCS data of nuclei with lower magnetogyric ratios than  $^1\text{H}$  have gained popularity in biomolecular NMR spectroscopy since those spins are less affected by relaxation enhancements caused by the paramagnetic center and, therefore, allow the NMR detection of spins closer to the metal ion.<sup>4</sup> Furthermore, the differences in the PCS values of, for example, the  $^1\text{H}^{\text{N}}$ ,  $^{15}\text{N}$ , and  $^{13}\text{C}'$  spins within a peptide group can be used to distinguish between different orientations of the peptide group with respect to the  $\chi$  tensor. Here we show that nonisotropic averaging of the nuclear chemical shift Hamiltonian arising from paramagnetic alignment results in residual anisotropic chemical shifts (RACS) that must be taken into account for an accurate analysis of PCS data of heteronuclear spins with pronounced chemical shift anisotropy (CSA).

The paramagnetically induced RACS are given by

$$\Delta\delta^{\text{RACS}} = \frac{B_0^2}{15\mu_0 k T} \sum_{ij} \delta_{ii}^{\text{CSA}} \cos^2 \theta_{ij} \Delta\chi_{jj} \quad (2)$$

where  $\delta_{ii}^{\text{CSA}}$  and  $\Delta\chi_{jj}$  are the Cartesian principal components of the nuclear CSA and the electronic  $\Delta\chi$  tensors, respectively;  $\cos \theta_{ij}$  values are the nine direction cosines between pairs of the principal axes;  $T$  is the temperature,  $B_0$  the magnetic field strength,  $k$  the Boltzmann constant, and  $\mu_0$  the induction constant.

CSA tensors of  $^1\text{H}^{\text{N}}$ ,  $^{15}\text{N}$ , and  $^{13}\text{C}'$  nuclei have been determined from  $\Delta\delta^{\text{RACS}}$  observed in the presence of a liquid crystalline medium,<sup>5</sup> from cross-correlated relaxation,<sup>6</sup> and from DFT calculations.<sup>7</sup> The problem of additional peak shifts in  $\Delta\delta^{\text{RACS}}$  measurements associated with a change in sample conditions between aligned and isotropic phase has been circumvented by interpolation of data recorded at different temperatures<sup>8</sup> and magic angle spinning of the aligned sample.<sup>9</sup> In the case of paramagnetic alignment, the

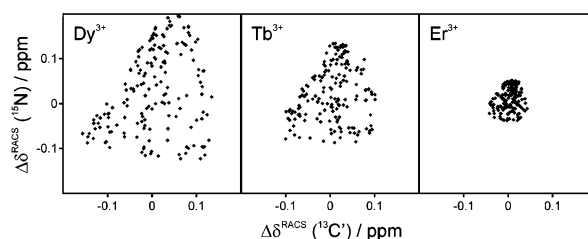


**Figure 1.** Predicted residual anisotropic chemical shifts (RACS) of  $^{15}\text{N}$  versus RACS of  $^{13}\text{C}'$  spins of N–C peptide groups of  $\epsilon 186$  in complex with  $\text{Dy}^{3+}$ ,  $\text{Tb}^{3+}$ , and  $\text{Er}^{3+}$ . The calculation used eq 2 with  $\Delta\chi$  tensor values determined from experimental  $^1\text{H}$  PCS data,<sup>11</sup> using the 1.8 Å X-ray structure of  $\epsilon 186$  (PDB code 1J53),<sup>12</sup> a magnetic field of 18.8 T (800 MHz), and a temperature of 25 °C. The CSA tensors of  $^1\text{H}^{\text{N}}$  and  $^{15}\text{N}$  were taken from the first row of Tables 3 and 4 in ref 5, and the CSA tensors of  $^{13}\text{C}'$  were calculated according to ref 7, with the isotropic chemical shifts of the complex of  $\epsilon 186$  with  $\text{La}^{3+}$ .

change in sample conditions is negligible if resonance frequencies are referenced to an otherwise identical sample containing a diamagnetic metal ion. The diamagnetic reference also cancels the contribution from the protein's intrinsic magnetic susceptibility to the alignment,<sup>10</sup> and from possible structural changes arising from metal binding.

For quantitative estimates of the paramagnetic RACS effect, we used  $\Delta\chi$  tensor parameters previously measured for the 30 kDa complex of the N-terminal domain of the  $\epsilon$  subunit,  $\epsilon 186$ , with the subunit  $\theta$  of *E. coli* DNA polymerase III containing one equivalent of  $\text{Dy}^{3+}$ ,  $\text{Tb}^{3+}$ , or  $\text{Er}^{3+}$ .<sup>11</sup> Figure 1 shows that, for strongly aligning metal ions at high magnetic fields (18.8 T),  $\Delta\delta^{\text{RACS}}$  can easily exceed 0.1 ppm for backbone carbonyl carbons and amide nitrogens. Due to the different orientations of the  $^{15}\text{N}$  and  $^{13}\text{C}'$  CSA tensors, the two values in a given peptide group are generally different. Although small compared to the largest paramagnetic shifts typically observable in these complexes,  $\Delta\delta^{\text{RACS}}$  is expected to exceed  $\Delta\delta^{\text{PCS}}$  for residues distant from the paramagnetic center (about 40 Å for  $\epsilon 186$ – $\theta$  at 800 MHz). Note that, in contrast to  $\Delta\delta^{\text{PCS}}$ ,  $\Delta\delta^{\text{RACS}}$  does not depend on the electron–nucleus distance  $r$  (eqs 1 and 2).

Figure 2 compares the observed paramagnetic shifts of carbonyl carbons in  $\text{Dy}^{3+}$ – $\epsilon 186$ – $\theta$  with the back-calculated values and also with the shifts calculated for the intrapeptide amide protons. Although, for most residues, the RACS correction is smaller than the difference of  $\Delta\delta^{\text{PCS}}$  between  $^1\text{H}^{\text{N}}$  and  $^{13}\text{C}'$ , it significantly improves the correlation between observed and calculated paramagnetic shifts of the  $^{13}\text{C}'$  spins (Figure 2c).

As expected,  $\Delta\delta^{\text{PCS}}$  is more similar between  $^{15}\text{N}$  and  $^1\text{H}^{\text{N}}$  than  $^{13}\text{C}'$  and  $^1\text{H}^{\text{N}}$  spins; nevertheless, the RACS correction improves the correlation for  $^{15}\text{N}$  spins similar as that for  $^{13}\text{C}'$  spins (Table 1). Improvements are also obtained for the  $\text{Tb}^{3+}$  and  $\text{Er}^{3+}$  complexes, where the degree of alignment amounts to 70 and 25% of that in the  $\text{Dy}^{3+}$  complex, respectively. The root-mean-square deviation (rmsd) between observed and predicted paramagnetic

<sup>†</sup> Australian National University.<sup>‡</sup> Ecole Normale Supérieure de Lyon.

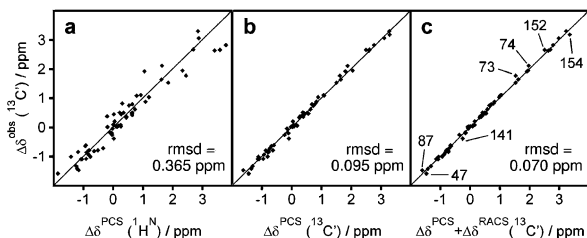


**Figure 2.** Correlation of observed paramagnetic shifts of backbone carbonyl  $^{13}\text{C}$  resonances of  $\text{Dy}^{3+}$ - $\epsilon 186$ - $\theta$ ,  $\Delta\delta^{\text{obs}}(^{13}\text{C})$  versus (a) the calculated pseudocontact shifts of the intrapeptide group backbone amide proton,  $\Delta\delta^{\text{PCS}}(^{1}\text{H}^{\text{N}})$ , (b) the calculated pseudocontact shift of the carbonyl resonances,  $\Delta\delta^{\text{PCS}}(^{13}\text{C}')$ , and (c) the paramagnetic shift of the carbonyl resonances calculated with RACS correction,  $\Delta\delta^{\text{PCS}} + \Delta\delta^{\text{RACS}}(^{13}\text{C}')$ . Paramagnetic shifts were measured as the chemical shift difference in 3D HNCO spectra recorded of the 0.6 mM complex between  $^{13}\text{C}/^{15}\text{N}$ -labeled  $\epsilon 186$  and unlabeled  $\theta$  containing  $\text{Dy}^{3+}$  and  $\text{La}^{3+}$ , respectively, at 18.8 T and 25  $^{\circ}\text{C}$ .<sup>11</sup> Rmsd values for the three correlations are indicated, and outliers ( $>0.1$  ppm deviation) in (c) are labeled with their residue number in  $\epsilon 186$ .

**Table 1.** Root Mean Square Deviation<sup>a</sup> between Observed and Predicted Paramagnetic Shifts of Backbone  $^{13}\text{C}$ ,  $^{15}\text{N}$ , and  $^{1}\text{H}^{\text{N}}$  in  $\epsilon 186$

metal	$\Delta\chi_{\text{ax}}$ ( $10^{-32}\text{ m}^3$ )	$\Delta\chi_{\text{m}}$ ( $10^{-32}\text{ m}^3$ )	X	$\Delta\delta^{\text{obs}}(\text{X}) - \Delta\delta^{\text{PCS}}(^{1}\text{H}^{\text{N}})$	$\Delta\delta^{\text{obs}}(\text{X}) - \Delta\delta^{\text{PCS}}(\text{X})$	$\Delta\delta^{\text{obs}}(\text{X}) - (\Delta\delta^{\text{PCS}} + \Delta\delta^{\text{RACS}}(\text{X}))$
$\text{Dy}^{3+}$	39.9	4.4	$^{13}\text{C}'$	0.365	0.095	0.070
			$^{15}\text{N}$	0.199	0.128	0.092
			$^{1}\text{H}^{\text{N}}$	0.064	0.064	0.064
$\text{Tb}^{3+}$	27.2	5.6	$^{13}\text{C}'$	0.237	0.065	0.057
			$^{15}\text{N}$	0.141	0.090	0.075
			$^{1}\text{H}^{\text{N}}$	0.046	0.046	0.045
$\text{Er}^{3+}$	−10.4	−4.3	$^{13}\text{C}'$	0.111	0.046	0.041
			$^{15}\text{N}$	0.086	0.082	0.073
			$^{1}\text{H}^{\text{N}}$	0.039	0.039	0.039

<sup>a</sup> Calculated in parts per million.

shifts did not decrease further when secondary structure specific CSA tensors<sup>5</sup> were used in eq 2. For amide protons, the RACS correction is negligible since the CSA of  $^{1}\text{H}^{\text{N}}$  (in ppm) is much smaller.<sup>13</sup> Therefore,  $^{1}\text{H}$  remains the most suitable spin for the determination of  $\Delta\chi$  tensor parameters from PCS data.

Notably, when including the  $\Delta\delta^{\text{RACS}}$  term, we observed a much faster convergence of the Echidna algorithm, which we recently developed for the automatic assignment of paramagnetic  $^{15}\text{N}$  HSQC spectra.<sup>11</sup> For most residues, the deviations between experimental and calculated paramagnetic shifts are now within the estimated experimental errors of 0.1 ppm for  $^{13}\text{C}'$  and  $^{15}\text{N}$  and 0.05 ppm for  $^{1}\text{H}^{\text{N}}$ . Other conceivable corrections to eq 1 arise from saturation of the electron magnetic moment at increased magnetic fields and from nonisotropic averaging of the electron–nuclear dipolar shift due to the paramagnetic alignment.<sup>14</sup> These effects are, however, proportional to  $\Delta\delta^{\text{PCS}}$  and of the order of  $10^{-3} \Delta\delta^{\text{PCS}}$  and, therefore, are only significant for nuclei in close proximity of the metal ion.

Six of the seven remaining deviations ( $>0.1$  ppm) highlighted in Figure 2c originate from residues in surface loops that are located

at or near crystal contacts. For all seven residues, the differences between observed and back-calculated paramagnetic shifts are consistent in sign and magnitude for all three  $^{1}\text{H}^{\text{N}}$ ,  $^{15}\text{N}$ , and  $^{13}\text{C}'$  spins, suggesting small translational displacements of these peptide groups in solution compared to their positions in the crystal structure. In contrast, no such consistency was apparent for the 19  $^{13}\text{C}'$  spins deviating by more than 0.1 ppm without the RACS correction (Figure 2b), 10 of which are part of regular secondary structure elements. For highly mobile loop regions,  $\Delta\delta^{\text{RACS}}$  would have to be scaled by an order parameter  $S < 1$ , analogous to the one defined for residual dipolar couplings.

These results demonstrate that once necessary RACS corrections have been taken into account, PCS data are exquisitely sensitive probes for structural details. It may thus become possible to interpret small yet significant differences in PCS observed for  $^{1}\text{H}^{\text{N}}$ ,  $^{15}\text{N}$ , and  $^{13}\text{C}'$  spins of the same peptide group in terms of its orientation (see Supporting Information). Furthermore, paramagnetically induced RACS effects can be used for structure validation in distant regions of the protein, where  $\Delta\delta^{\text{PCS}}$  is small.

**Acknowledgment.** M.J. thanks the Humboldt Foundation for a fellowship. Financial support from the Australian Research Council for a Federation Fellowship for G.O. and the 800 MHz NMR spectrometer at ANU is gratefully acknowledged.

**Supporting Information Available:** Plot of experimental paramagnetic shifts observed for  $^{1}\text{H}^{\text{N}}$ ,  $^{13}\text{C}'$ , and  $^{15}\text{N}$  spins of  $\epsilon 186$  in complex with  $\theta$  in the presence of  $\text{Dy}^{3+}$  versus amino acid sequence. This material is available free of charge via the Internet at <http://pubs.acs.org>.

## References

- (1) Allegrozzi, M.; Bertini, I.; Janik, M. B. L.; Lee, Y.-M.; Liu, G.; Luchinat, C. *J. Am. Chem. Soc.* **2000**, *122*, 4154–4161.
- (2) (a) Banci, L.; Bertini, I.; Cremonini, M. A.; Gori-Savellini, G.; Luchinat, C.; Wüthrich, K.; Güntert, P. *J. Biomol. NMR* **1998**, *12*, 553–557. (b) Gaponenko, V.; Sarma, S. P.; Altieri, A. S.; Horita, D. A.; Li, J.; Byrd, R. A. *J. Biomol. NMR* **2004**, *28*, 205–212.
- (3) Pintacuda, G.; Keniry, M. A.; Huber, T.; Park, A. Y.; Dixon, N. E.; Otting, G. *J. Am. Chem. Soc.* **2004**, *126*, 2963–2970.
- (4) (a) Serofani, S. D. B.; Brownlee, R. T. C.; Sadek, M.; Wedd, A. G. *Inorg. Chem.* **1995**, *34*, 3942–3952. (b) Babini, E.; Bertini, I.; Capozzi, F.; Felli, I. C.; Lelli, M.; Luchinat, C. *J. Am. Chem. Soc.* **2004**, *126*, 10496–10497.
- (5) Cornilescu, G.; Bax, A. *J. Am. Chem. Soc.* **2000**, *122*, 10143–10154.
- (6) Loth, K.; Peluppesy, P.; Bodenhausen, G. *J. Am. Chem. Soc.* **2005**, *127*, 6062–6068.
- (7) Markwick, P. R. L.; Sattler, M. *J. Am. Chem. Soc.* **2004**, *126*, 11424–11425.
- (8) (a) Cornilescu, G.; Marquardt, J. L.; Ottinger, M.; Bax, A. *J. Am. Chem. Soc.* **1998**, *120*, 6836–6837. (b) Boyd, J.; Redfield, C. *J. Am. Chem. Soc.* **1999**, *121*, 7441–7442.
- (9) Kurita, J.; Shimahara, H.; Utsunomiya-Tate, N.; Tate, S. *J. Magn. Reson.* **2003**, *163*, 163–173.
- (10) Ottinger, M.; Tjandra, N.; Bax, A. *J. Am. Chem. Soc.* **1997**, *119*, 9825–9830.
- (11) Schmitz, C.; John, M.; Park, A. Y.; Dixon, N. E.; Otting, G.; Pintacuda, G.; Huber, T. Submitted.
- (12) Hamdan, S.; Carr, P. D.; Brown, S. E.; Ollis, D. L.; Dixon, N. E. *Structure* **2002**, *10*, 535–546.
- (13) Tjandra, N.; Bax, A. *J. Am. Chem. Soc.* **1997**, *119*, 8076–8082.
- (14) (a) Bertini, I.; Felli, I. C.; Luchinat, C. *J. Magn. Reson.* **1998**, *134*, 360–364. (b) Bertini, I.; Luchinat, C.; Parigi, G. *Prog. NMR Spectrosc.* **2002**, *40*, 249–273.

JA0564259